ILASS 2008
Sep. 8-10, 2008, Como Lake, Italy

Paper ID ILASS08-9-4

BINARY COLLISION BETWEEN UNEQUAL SIZED DROPLETS. A NUMERICAL INVESTIGATION.

N. Nikolopoulos[1], A. Theodorakakos[2] and G. Bergeles[3]

[1] Electronic mail:niknik@fluid.mech.ntua.gr
[2] Electronic mail:andreas@fluid.mech.ntua.gr
[3] Author to whom correspondence should be addressed. Electronic mail:bergeles@fluid.mech.ntua.gr. Telephone: +302107721058. Fax.: +302107723616. Postal address: Nat. Technical University of Athens, Department of Mehanical Engineereing, 5 Heroon Polytechniou, Zografos, 15710, Athens, Greece.

ABSTRACT

The paper presents a numerical investigation of the collision of two unequal sized droplets in a gaseous phase. The numerical method is based on the finite volume numerical solution of the Navier-Stokes equations, in their axi-symmetric formulation, expressing the flow field of the two phases, liquid and gas, coupled with the Volume of Fluid Method (V.O.F) for tracking the liquid-gas interfaces; a recently developed adaptive local grid refinement technique is used in order to track more accurately the liquid-gas interface. The results are compared with available experimental data and indicate the outcome of the collision (coalescence or separation), the interchange between droplet kinetic energy and surface energy with the associated viscous dissipation, the maximum deformation of the droplet, whilst the method gives details of the flow and pressure fields not hitherto available. Furthermore, the penetration of smaller droplet's mass within the merged liquid mass, is investigated.

INTRODUCTION

The binary droplet collision is of engineering and environmental importance in a variety of applications such as fuel direct injection into internal combustion engines, rain formation and spray cooling or coating. Because of the complex physical mechanisms involved in such process, experimental investigations alone may not be able to describe the governing physics. Adam et al.[1] were the first to investigate experimentally binary droplet collision, using water droplets in air, at atmospheric pressure. These studies have been conducted because of meteorological interest (rain-drops). Later, Park [2], Brazier-Smith et al. [3], Ashgriz and Poo [4] extended the experimental study on the collision of rain drops, advancing the understanding on the formation and growth of rain droplets. The main governing parameters of the binary collision are the droplet Weber number (We) and the Ohnesorge number (Oh). Nevertheless, the collision outcome depends also on the physical properties (density, viscosity) of both liquid and gas phases and the surface tension of the liquid in the gas phase, as also, for the present case, by the diameter ratio of the two droplets.

Most experimental studies focused attention on the binary collision between equal-sized droplets, without considering the effect of the droplet size ratio. The present investigation studies numerically the central collision of water droplets for various Weber and Ohnesorge numbers considering the effect of droplet size ratio on the collision between non-equal sized droplets. The Navier-Stokes equations with the introduction of a volumetric force due to surface tension effects are solved numerically by the finite volume methodology; the numerical solution employs a new adaptive local grid refinement technique, whilst V.O.F methodology is used for the tracking of the liquid –gas interfaces. It should be mentioned that, the aforementioned equations are coupled with an additional equation for the identification of the smaller droplet's mass distribution within the liquid phase after the coalescence of the two initial droplets.

2. The mathematical problem

2.1. The V.O.F function α

The flow induced by the binary collision of two droplets is considered as two-dimensional axi-symmetric, incompressible and laminar; the two-phase flow (phase 1 is the liquid phase, *i.e.* the two droplets, phase 2 is the surrounding gas phase) is mathematically expressed by the Navier-Stokes equations and the continuity equation with extra terms which take into account the forces due to surface tension. For identifying each phase separately a volume fraction, denoted by α, is introduced following the Volume of Fluid Method (V.O.F) of Hirt and Nichols [5]. In the V.O.F methodology the volume fraction α is defined as:

$$\alpha = \frac{\text{Volume of fluid 1 (liquid phase)}}{\textit{Total}\ \text{volume of the control volume}} \qquad (1)$$

The values of density ρ and dynamic viscosity μ are calculated using linear interpolation between the values of the two phases weighted with the volume fraction α,:

$$\rho=\alpha\rho_{liq}+(1-\alpha)\rho_{gas}$$
$$\mu=\alpha\mu_{liq}+(1-\alpha)\mu_{gas} \qquad (2)$$

, where the α-function is equal to:

$$\alpha(x,t)=\begin{cases}1, & \text{for the point (x,t) inside the liquid phase}\\ 0, & \text{for the point (x,t) inside the gas phase}\\ 0<a_{\delta}<1, & \text{for the point (x,t) inside the transitional area between the two phases}\end{cases} \quad (3)$$

For a single droplet splashing onto a wall film, the V.O.F methodology has been successfully applied previously and the method is described in more detail in Nikolopoulos et al. [8,9].

Following Hirt and Nichols [5], the location of the interface is calculated on the assumption that the material derivative of the V.O.F function α is zero:

$$\frac{\partial a}{\partial t}+\vec{u}\cdot\nabla a=0 \quad (4)$$

The momentum equations expressing both phases are written in the form

$$\frac{\partial(\rho\vec{u})}{\partial t}+\nabla\cdot(\rho\vec{u}\otimes\vec{u}-\vec{T})=\rho\vec{g}+\vec{f}_{\sigma} \quad (5)$$

, where $\vec{u}$ is the velocity vector, t is time, $\vec{T}$ is the stress tensor and f_σ is the volumetric force due to surface tension. The value of f_σ is equal to $f_{\sigma}=\sigma\cdot\kappa\cdot(\nabla a)$, where σ is the numerical value of the surface tension (for immiscible fluids the value is always positive) and κ is the curvature of the interface region, Brackbill [6].

A recently developed adaptive local grid refinement technique, proposed by Theodorakakos and Bergeles [7] and employed in Nikolopoulos et al. [8,9], is used in order to enhance accuracy in the areas of interest (i.e the interface between the liquid and gas phases), securing a low computational cost. The gas-liquid interface is characterized by high flow gradients, thus the computational cells in this region are dub-divided to a prescribed number of layers in both sides of the interface, in order to achieve the desired maximum resolution level. In most cases five levels of local refinement are used and a new locally refined mesh is created every 10 time steps following the liquid-gas interface motion and distortion. As a result, the interface always lies in the densest grid resolution.

2.2. The numerical solution procedure

Except for the V.O.F function –α- transport equation, an additional transport equation for the concentration of the material originating from the smaller droplet in the liquid phase (after droplets coalescence), Eq. (6), is solved.

$$\frac{D(C)}{Dt}=0 \quad (6)$$

, where C is the mass of the smaller droplet in the whole liquid mass.

$$C=\frac{\text{Mass of smaller droplet}}{\text{Total liquid mass of the control volume}} \quad (7)$$

The maximum value of C is equal to 1, if the numerical cell is covered only by mass originating from the smaller droplet's initial mass, equal to 0, if the numerical cell is covered only by mass originating from the larger droplet's initial mass, whilst any intermediate value declares the percentage of mass originating from the smaller droplet's initial mass.

2.3. Numerical details

The main parameters of the binary collision between unequal sized droplets process are the smaller droplet's diameter D_s, the larger droplet's diameter D_l and their corresponding initial impact velocities $\vec{U}_s$ and $\vec{U}_l$; other significant parameters are the density ρ and viscosity μ of the liquid and gas phases as also the surface tension σ. These variables are grouped in dimensionless parameters, namely the Weber and the Ohnesorge numbers. Furthermore, the relative velocity of the impacting droplets $\vec{U}_{rel}=\vec{U}_s-\vec{U}_l$ and the dimensionless time $T = t\,U_{rel}/D_s$ are introduced. The relevant non-dimensional parameters for this problem, i.e., the Weber (We) number, and Ohnesorge (Oh) number are defined, respectively, as:

$$We=\frac{\rho_{liq}\cdot D_s\cdot(U_{rel})^2}{\sigma},\quad Oh=\frac{\mu_{liq}}{\sqrt{\rho_{liq}\cdot\sigma\cdot D_s}} \quad (8)$$

The computational domain is shown in Fig. 1. The solution domain is axi-symmetric (around the X axis) and the droplets are initially placed one diameter apart. The experimental investigation reported by Ashgriz and Poo[4] will form the basis of the present numerical simulation.

For the cases A to D examined, shown in table 1, the "base" grid which was employed, consisted of 1350 numerical cells; a rectangular computational domain covering a space of $X_{tot}=11.5\ D_l$, $Y_{tot}=1.91\ D_l$ in the X and Y dimensions respectively, is used. Five levels of local grid refinement are created, resulting to a maximum number of 13000 numerical cells. The maximum refinement resulted to a cell size of $D_l/250$. In order to investigate the grid dependency of the results, cases A and B were also simulated using six levels of local refinement, resulting in a minimum cell size equal to $D_o/500$ and gave almost the same results with that of the coarser grid. The numerical simulation for these cases has lasted around 1 ½ days on a Pentium 4 with a 2.4GHz processor.

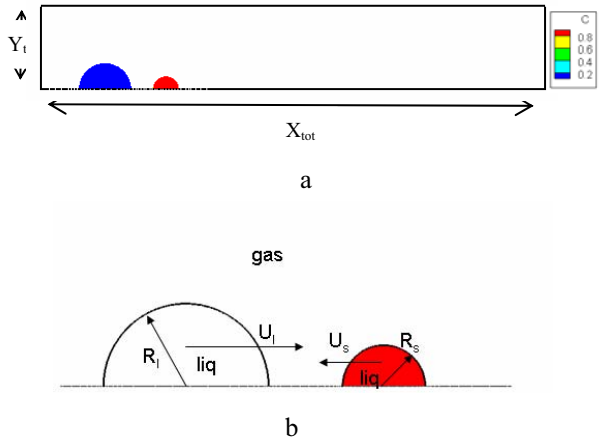

Fig.1. a) The computational domain, b) definition of basic parameters.

Table 1: Conditions of cases examined.

Case	D_s(mm)	D_l(mm)	$\Delta=D_s/D_l$	We	Oh
A	0.626	1.044	0.60	25	0.0047
B	0.626	1.252	0.5	56.04	0.0047
C	0.626	1.252	0.5	56.04	0.047
D	0.626	0.626	1	56.04	0.0047

3. Collision of two droplets of unequal sizes

3.1. Effect of We number.

Figure 2 shows a sequence of photographs from the experiments of Ashgriz and Poo [4] and their corresponding simulation of the two colliding droplets, for low We number impact, case A. The extent of deformation and the shape of the two colliding droplets at various time instants after contact deduced from the experimental and numerical data are in very good agreement. In this case, the experiments suggest that coalescence between the two droplets occurs. During the initial stages of impact, the liquid in both droplets spreads radially in the plane normal to the centre-to-centre line, Fig. 2, t=1.98ms, generating a disk like droplet. Afterwards, the coalesced mass contracts towards the symmetry axis, due to surface tension forces, creating an elongated cylinder in the centre-to-centre line direction, Fig.2, t=3.00ms. The final result of the impact is the permanent coalescence of the two initial droplets. From the concentration contour of Fig. 2 it is evident that the liquid mass originating from the smaller droplet spreads on the external part of the larger droplet, whilst liquid of the larger droplet penetrates well into the central part of the smaller droplet; as time passes the liquid of the smaller droplet is convected into the mass of the larger droplet.

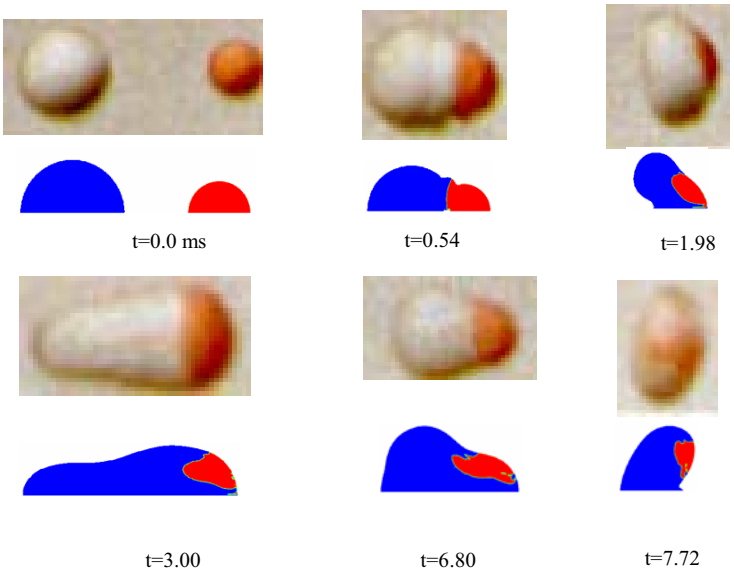

Fig. 2. Time evolution for case A.

Increasing the We number of the impact (case B), again liquid spreads radially and later contracts towards the symmetry axis, Fig.3, t=0.88ms, but during the elongation of the formed cylinder along the symmetry axis, a ligament between the two opposite moving boundary droplets is created, Fig. 3, t=5.40ms; the ligament breaks up from the one side leaving one secondary droplet and afterwards by receding merges with the other boundary droplet creating the second secondary droplet. Thus, two secondary droplets of unequal size are formed, Fig. 3, t=7.00ms. The smaller has a volume of around 33.84% of the total volume of the initial droplets, whilst the larger a volume equal to around 66.16%. The larger and the smaller droplets have a diameter equal to 93% and 74.4% of D_l respectively. The extent of deformation and the shape of the two colliding droplets at various time instants after contact deduced from the experimental and numerical data are in very good agreement. The liquid mass originating from the smaller initial droplet moves more out on the surface of the larger droplet and the larger droplet penetrates more into the central core of the smaller droplet at respective times in case B, in the merged liquid mass, than in case A, due to the higher momentum, since the droplets have a greater relative velocity. The smaller secondary droplet is located at the side of the initial large droplet and mainly it consists of liquid from the large initial droplet; the larger secondary droplet, which is located at the side of the initial small droplet consists of liquid of the initial large droplet, liquid mainly found at the central part of the droplet, whilst liquid from the initial small droplet is found on the periphery of the droplet.

From the time evolution of cases A and B, it is evident that as the We number of impact increases, the coalesced mass begins to separate reflexively, as in the case of head-on collisions, whilst the penetration of the liquid mass originating from the smaller droplet, inside the merged mass increases peripherally.

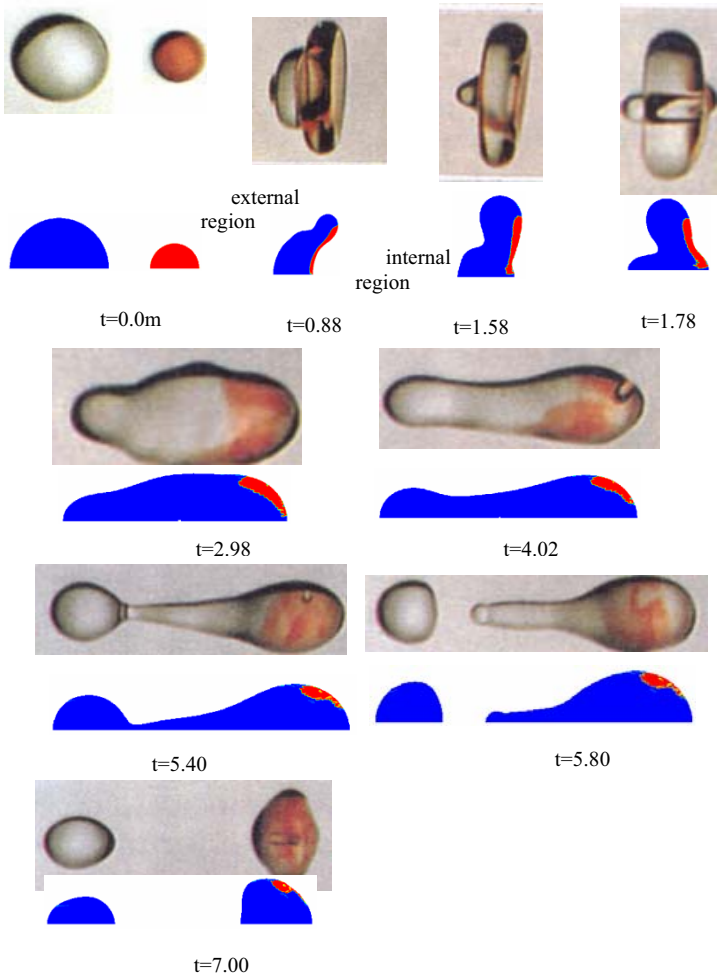

Fig. 3. Time evolution for case B

As the droplets approach each other the pressure in the air gap between the two droplets increases, the droplets' common area flattens and the gas between the droplets is squeezed out

creating a sheet of a gas jet between the two droplets (Fig. 4, t=0.24 ms.). Surrounding air is entrained into the gas jet and on the two sides of this gas jet two vortex rings, attached to the upper liquid surface of each droplet are formed; these vortex rings remain attached there, during the approaching phase of the collision process. It is of interest to notice the continuity of the velocity field through the gas liquid interface, as also the well-defined liquid gas interfaces, an indication of the non-diffusive character of the CICSAM discretisation scheme, Ubbink and Issa [10]. Figure 4 also shows the pressure distribution within the droplets during collision for case B. In case A, the value of the maximum gas jetting velocity is around 874% (626%, case B) of the droplet's impact velocity, whilst the maximum liquid jetting velocity is around 373% (326%, case B) of the droplet's impact velocity. In case A values of pressure coefficient C_p up to 923% (517%, case B) of the initial total droplet's kinetic energy (based on the relative velocity of droplets, $C_p=\Delta P/(0.5\ \rho_{liq}\ (U_{rel})^2\ )$ at the front stagnation point are developed with the maximum pressure developing at the periphery of the droplet-droplet contact area. Pressure builds up very fast, and then decreases with time (Fig. 4); the strength of the vortex rings has a minimum value at the time of maximum deformation, maximum value at the first stages of the collision, whilst changes sign during the receding phase, as air accelerates to fill in the gap which opens between the two separating droplets (t>5.60ms).

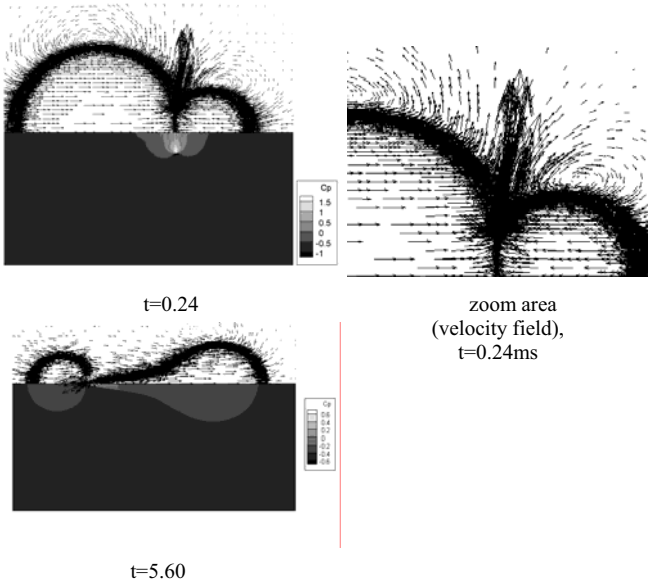

Fig. 4. Pressure and velocity field evolution for Case B.

Finally, in Fig 5, the entrapment of an air bubble during the initial stages of impact, for case B, is shown. Ashgriz and Poo [4], reported in their experimental work the entrapment of microbubbles, during the coalescence of two unequal sized droplets with a size ratio of 0.65 at We=30. Despite the fact that this case is not reasonably close to the predicted case B, in which the size ratio is 0.5 and the We number is 56, again entrapment of gas phase is predicted. Premnath and Abraham [11] predicted numerically the entrapment of a microbubble for a size ratio of 0.5 and a We number equal to 20. In case B, the volume of the bubble is equal to around 0.000152% of the initial liquid volume of both droplets.

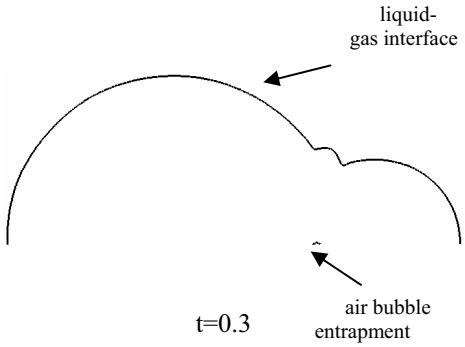

Fig. 5. Bubble entrapment

3.2. Effect of Oh number.

Jiang et al. [12] were the first who investigated the importance of the physical properties of liquid and gas phases on the collision outcome of binary collision. In particular, they pointed out that the liquid droplet viscosity increases the transition We number between coalescence and reflexive separation. Ohnesorge number represents the relative importance of viscous forces due to internal motion inside the droplet compared to surface tension forces. The Oh number is varied by changing the dynamic viscosity of the liquid phase and keeping constant the other parameters. Case C was examined, in comparison to case B, in order to investigate the effect of Oh number on the evolution of binary collision phenomenon between unequal sized droplets. Fig. 6 presents the time evolution of case C. Comparing case B (Fig. 2) and C (Fig. 6), it is evident that in contrast to case B, in case C no reflexive separation occurs and the merged droplet remains coalesced, Fig. 6, t=7.00ms. This behavior is consistent with the experimental result of Jiang et al. [12]. In addition comparing the contour of smaller droplet's mass concentration inside the merged liquid mass for cases B and C, Fig. 2 and 6, at respective times t=1.58ms and t=1.78ms, it is deduced that the smaller droplet's mass diffuses less inside the merged mass in case C. This can be attributed to the greater viscosity which damps out velocity gradients in case C (greater liquid viscosity) than in case B.

In case C, the value of the maximum gas jetting velocity is around 503% (626%, case B) of the droplet's impact velocity, whilst the maximum liquid jetting velocity is around 280% (326%, case B) of the droplet's impact velocity. In case C values of pressure coefficient C_p up to 401% (517%, case B) of the initial total droplet's kinetic energy (based on the relative velocity of droplets, $C_p=\Delta P/(0.5\ \rho_{liq}\ (U_{rel})^2\ )$ at the front stagnation point are developed. For case C the reduced values in the pressure and the velocity of the induced flow field are consistent with the increase of viscous dissipation.

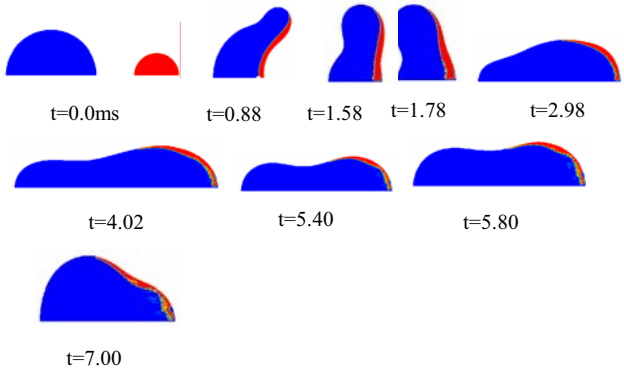

Fig. 6. Time evolution for case C.

3.4. Effect of droplet size ratio.

Case D was examined in order to identify the effect of droplet size ratio on the evolution of the phenomenon. Fig. 7 presents the time evolution of the central impact of two equal sized droplets in contrast to case B, keeping We and Oh numbers constants. Comparing figures 3 and 7, t=0.88ms, it is evident that in case D in contrast to case B, the two initial droplets deform symmetrically, as expected; furthermore, in case D, during the receding phase of the merged liquid mass towards the symmetry axis, the axial stretching is higher, Fig.7, t=2.98ms and the in-between formed ligament, separates from the edges of the two opposite moving boundary droplets , Fig. 7, t=3.20ms. Later, this ligament due to surface tension force, oscillates until it reaches an almost spherical shape, Fig. 7, t=4.02ms. Hence, unlike in case B, one secondary droplet and two boundary droplets are produced. Each of the boundary secondary droplets has a volume equal to around 34.63%, whilst the intermediate a volume equal to around 30.74% of the initial liquid volume of both droplets. Each of the boundary droplets has a diameter equal to 88.4% of the initial droplet's diwmeter, whilst the intermediate a diameter equal to 85%. Consequently, collision between equal-sized droplets, produces more secondary droplets, than the respective one between unequal-sized droplets, with the same Weber and Ohnesorge numbers.

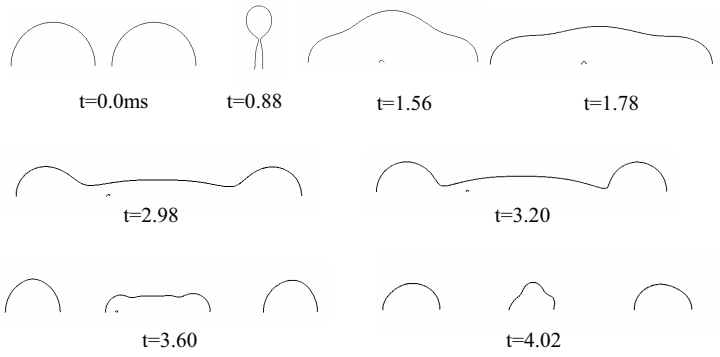

Fig. 7. Time evolution for case D.

4. Conclusions

The flow field arising from the binary droplet collision between unequal sized water droplets was numerically studied using a finite volume methodology incorporating the volume of fluid (V.O.F) methodology and an adaptive local grid refinement technique. A higher order discretisation scheme was found necessary for the numerical solution of the transport equation for the V.O.F indicator in order to accurately track the droplet-gas interface. The use of an additional equation for the concentration of the liquid mass originating from the smaller droplet in the liquid phase, allowed the prediction of the mixing process of the collision of the two droplets. The numerical results agree reasonably well with the corresponding experimental data. The V.O.F method was capable of predicting the details of the flow, like gas bubble entrapment, droplet deformation, air and liquid jetting and satellite droplet formation. The collision of unequal sized droplets in the case of reflexive separation leads to the formation of a smaller number of satellite droplets, compared to equal sized droplet collision. The smaller droplet upon collision stretches onto the surface of the larger droplet whilst the larger droplet penetrates well into the central part of the smaller droplet.

ACKNOWLEDGMENT

The financial support of the EU under contract N^{o} ENK6-2000-00051 is acknowledged.

REFERENCES

[1] J.R.Adam, N.R.Lindblad, and C.D. Hendricks. The collision, coalescence, and disruption of water droplets. J. Appl. Phys. 39, 173, 1968.

[2] R.W.Park. Behavior of water drops colliding in humid nitrogen. PhD thesis, Department of Chemical Engineering, The University of Wisconsin, 1970.

[3] P.R. Brazier-Smith, S.G. Jennings and J. Latham. The interaction of falling water drops: coalescence. Proc.R. Soc. Lond. A 326, 393, 1972.

[4] N. Ashgriz and J.Y. Poo. Coalescence and separation in binary collision of liquid drops. J.Fluid.Mech. 221,pp. 183-204, 1990.

[5] C.W. Hirt and B.D. Nichols. Volume of fluid (VOF) method for the dynamics of free boundaries. J.Comput.Phys., Vol.39, pp. 201-225, 1981.

[6] J.U. Brackbill, D.B. Kothe, and C. Zemach. A continuum method for modelling surface tension, Journal of Computational Physics, 1992;Vol. 100, No. 2:335-354.

[7] A. Theodorakakos, G. Bergeles. Simulation of sharp gas-liquid interface using VOF method and adaptive grid local refinement around the interface. Int. J. Numer. Meth. Fluids, 45, pp. 421-439, 2004.

[8] N. Nikolopoulos, A. Theodorakakos, G. Bergeles. Normal impingement onto a wall film: a numerical investigation. Int. Jour, Heat and Fluid Flow, 26, pp. 119-132, 2005.

[9] N. Nikolopoulos, A. Theodorakakos, G. Bergeles. Three-dimensional numerical investigation of a droplet impinging normally onto a wall film. Journal Comp. Phys, 2007.

[10] O. Ubbink, R.I. Issa. A Method for Capturing Sharp Fluid Interfaces on Arbitrary Meshes. Journal of Computational Physics, Vol 153, Issue 1, pp. 26-50, 1999.

[11] K. Premnath, J. Abraham. Simulation of binary drop collisions with a multiple-relaxation-time lattice-Boltzmann model. Phys. Fluids, 17,122105, 2005.

[12] Y.J. Jiang, A. Umemura and C.K. Law. An experimental investigation on the collision behaviour of hydrocarbon droplets. J.Fluid.Mech. 234,171, 1992.